KEY ROLE OF THE RESIN LAYER THICKNESS IN THE LABILITY OF COMPLEXES MEASURED BY DGT

SUPPORTING INFORMATION

Sandrine Mongin^a, Ramiro Uribe^{a,d}, Jaume Puy^{a*}, Joan Cecília^b, Josep Galceran^a, Hao Zhang^c and William Davison^c

^aDepartament de Química, ^bDepartament de Matemàtica, Universitat de Lleida, Rovira Roure 191, 25198, Lleida, Spain

^cLancaster Environment Centre, Lancaster University, Lancaster, United Kingdom

^dDepartamento de Física, Universidad del Tolima, Ibagué, Colombia

* Corresponding author. e-mail address: jpuy@quimica.udl.es, Phone 34 973 702529, Fax 34 973 702924

Journal: Environmental Science and Technology

Date: 27-04-2011

Document with 25 pages, 7 figures and 1 Table

Supplementary information available:

Section 1: Numerical Simulation of a DGT Sensor.

Section 2: Concentration profiles in a DGT experiment.

Section 3: Experimental Section.

Section 4: Additional figures.

Section 5.- Formulation of the Cd-NTA speciation in a DGT sensor as a system with only one complex and ligand species.

Section 6.- Parameter values of all the figures of the manuscript

1.- Numerical Simulation of a DGT Sensor

1.1.- The Model

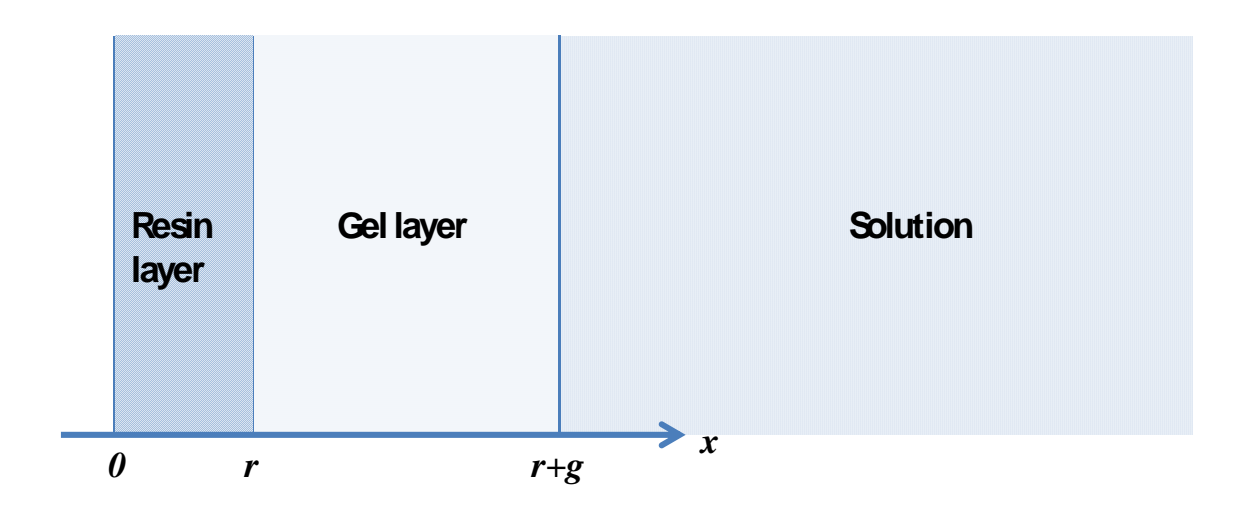


Figure SI-1. Schematic representation of a DGT device.

The model formulation coincides with that of (Lehto et al. 2006) and (Tusseau-Vuillemin et al. 2003).

Let D_i and $D_{i,R}$ stand for the diffusion coefficients of species i in the diffusive gel or in the resin domain, respectively and let c_i stand for the concentration of species i at a given spatial position x and time t. Total concentrations are denoted as $c_{T,i}$.

. The transport equations for the different species can be written as:

• For the metal in the gel layer and in the resin layer:

$$\frac{\partial c_{\mathrm{M}}}{\partial t} = D_{\mathrm{M,R}} \frac{\partial^{2} c_{\mathrm{M}}}{\partial x^{2}} - k_{\mathrm{a}} c_{\mathrm{M}} c_{\mathrm{L}} + k_{\mathrm{d}} c_{\mathrm{ML}} - k_{\mathrm{a,R}} c_{\mathrm{M}} c_{\mathrm{R}} + k_{\mathrm{d,R}} c_{\mathrm{MR}}, \quad \text{if} \quad 0 < x < r$$
 (SI-1)

$$\frac{\partial c_{\mathrm{M}}}{\partial t} = D_{\mathrm{M}} \frac{\partial^{2} c_{\mathrm{M}}}{\partial x^{2}} - k_{\mathrm{a}} c_{\mathrm{M}} c_{\mathrm{L}} + k_{\mathrm{d}} c_{\mathrm{ML}}, \quad \text{if} \quad r < x < r + g$$
(SI-2)

• For the ligand:

$$\frac{\partial c_{L}}{\partial t} = \begin{cases} D_{L,R} \\ D_{L} \end{cases} \frac{\partial^{2} c_{L}}{\partial x^{2}} + k_{a} c_{M} c_{L} - k_{d} c_{ML}, \quad \text{if} \quad 0 < x < r + g$$
(SI-3)

where the curly bracket indicates that $D_{\rm L,R}$ applies when 0 < x < r and $D_{\rm L}$ applies when r < x < r + g

 For the complex (assuming the same diffusion coefficient for complex and ligand):

$$\frac{\partial c_{\text{ML}}}{\partial t} = \begin{cases} D_{\text{L,R}} \\ D_{\text{L}} \end{cases} \frac{\partial^2 c_{\text{ML}}}{\partial x^2} + k_{\text{a}} c_{\text{M}} c_{\text{L}} - k_{\text{d}} c_{\text{ML}}, & \text{if } 0 < x < r + g \end{cases}$$
(SI-4)

• For the resin sites free (R) or occupied (MR):

$$\frac{\partial c_{\rm R}}{\partial t} = -k_{\rm a,R}c_{\rm M}c_{\rm R} + k_{\rm d,R}c_{\rm MR}, \quad \text{if} \quad 0 < x < r \tag{SI-5}$$

$$\frac{\partial c_{\text{MR}}}{\partial t} = +k_{\text{a,R}} c_{\text{M}} c_{\text{R}} - k_{\text{d,R}} c_{\text{MR}}, \quad \text{if} \quad 0 < x < r$$
 (SI-6)

There are no resin sites in the gel domain: $c_R(x,t) = c_{MR}(x,t) = 0$ for r < x < r + g.

Initial conditions correspond to the absence of metal and ligand in the sensor:

$$c_{\rm M}(x,0) = c_{\rm L}(x,0) = c_{\rm ML}(x,0) = 0$$
, if $0 < x < r + g$ (SI-7)

$$c_{MR}(x,0) = 0$$
 if $0 < x < r$ (SI-8)

$$c_{R}(x,0) = c_{T,R}$$
 if $0 < x < r$ (SI-9)

where $c_{\rm T,R}$ denotes the total concentration of resin sites (free or occupied).

Boundary conditions at x = r + g correspond to bulk concentrations:

$$c_{\rm M}(r+g,t) = c_{\rm M}^*, \quad c_{\rm L}(r+g,t) = c_{\rm L}^*, \quad c_{\rm ML}(r+g,t) = c_{\rm ML}^*$$
 (SI-10)

Boundary conditions at x = r:

at the gel-resin interface $c_{\rm M}(x,t), c_{\rm L}(x,t)$, and $c_{\rm ML}(x,t)$ and their fluxes must be continuous, that is

$$c_{\rm M}(r^{-},t) = c_{\rm M}(r^{+},t), \quad c_{\rm L}(r^{-},t) = c_{\rm L}(r^{+},t), \quad c_{\rm ML}(r^{-},t) = c_{\rm ML}(r^{+},t) \text{ and}$$
 (SI-11)

$$D_{\mathrm{M,R}} \frac{\partial c_{\mathrm{M}}}{\partial x} \Big|_{r^{-}} = D_{\mathrm{M}} \frac{\partial c_{\mathrm{M}}}{\partial x} \Big|_{r^{+}}, \quad D_{\mathrm{L,R}} \frac{\partial c_{\mathrm{L}}}{\partial x} \Big|_{r^{-}} = D_{\mathrm{L}} \frac{\partial c_{\mathrm{L}}}{\partial x} \Big|_{r^{+}}, \quad D_{\mathrm{L,R}} \frac{\partial c_{\mathrm{ML}}}{\partial x} \Big|_{r^{-}} = D_{\mathrm{L}} \frac{\partial c_{\mathrm{ML}}}{\partial x} \Big|_{r^{+}}$$
(SI-12)

The continuity of the concentrations indicates that no Donnan effects are considered, so that charge effects of the resin are screened by the supporting electrolyte.

Boundary conditions at x = 0 stem from non-flux conditions:

$$\frac{\partial c_{\rm M}}{\partial x}\bigg|_{x=0} = \frac{\partial c_{\rm L}}{\partial x}\bigg|_{x=0} = \frac{\partial c_{\rm ML}}{\partial x}\bigg|_{x=0} = 0. \tag{SI-13}$$

Eqns. (SI-1)-(SI-6) with the initial conditions (SI-7 to SI-9) and boundary value problem (SI-10-SI-13) form a system of equations for $c_{\rm M}(x,t),\ c_{\rm L}(x,t),\ c_{\rm ML}(x,t),\ c_{\rm R}(x,t)$ and $c_{\rm MR}(x,t)$.

It could be useful to introduce the total ligand concentration, $c_{\rm T,L}$. Adding equations (SI-3) and (SI-4), the transport equation for $c_{\rm T,L}$ becomes:

$$\frac{\partial c_{\text{T,L}}}{\partial t} = \begin{cases} D_{\text{L,R}} \\ D_{\text{L}} \end{cases} \frac{\partial^2 c_{\text{T,L}}}{\partial x^2}, \quad \text{if} \quad \begin{cases} 0 < x < r \\ r < x < r + g \end{cases}, \tag{SI-14}$$

with initial and boundary conditions given by:

$$c_{\text{T,L}}(x,0) = 0, \quad \frac{\partial c_{\text{T,L}}}{\partial x}\Big|_{x=0} = 0, \quad c_{\text{T,L}}(r+g,t) = c_{\text{T,L}}^* \quad \text{and}$$
 (SI-15)

$$c_{\text{T,L}}(r^{-},t) = c_{\text{T,L}}(r^{+},t), \quad D_{\text{L,R}} \frac{\partial c_{\text{T,L}}}{\partial x} \bigg|_{r^{-}} = D_{\text{L}} \frac{\partial c_{\text{T,L}}}{\partial x} \bigg|_{r^{+}}$$
 (SI-16)

Additionally, we can introduce the total resin concentration:

$$c_{\rm R}(x,t) + c_{\rm MR}(x,t) = c_{\rm T.R}$$
 (SI-17)

The addition of Eqs. (SI-5) and (SI-6) indicates, as physically expected, that $c_{\rm T,R}$ is time independent. Thus the finding of $c_{\rm M}(x,t), \ c_{\rm L}(x,t), \ c_{\rm ML}(x,t), \ c_{\rm R}(x,t)$ and $c_{\rm MR}(x,t)$ can be reduced to the finding of $c_{\rm M}(x,t), \ c_{\rm L}(x,t), \ c_{\rm T,L}(x,t), \ {\rm and} \ c_{\rm R}\left(x,t\right)$ in the domain 0 < x < r + g.

1.2.- Dimensionless Reformulation

Let us reformulate the problem in terms of dimensionless functions and normalized variables.

Let z be the spatial normalized variable. Its relationship with x and with its derivatives is:

$$z = \frac{x}{\sqrt{D_{\rm M}}} \rightarrow \frac{\partial^2}{\partial z^2} = \frac{1}{D_{\rm M}} \frac{\partial^2}{\partial x^2}$$
 (SI-18)

Then

$$r^* = \frac{r}{\sqrt{D_{\rm M}}}, \quad g^* = \frac{r+g}{\sqrt{D_{\rm M}}}$$
 (SI-19)

The dimensionless diffusion coefficients:

$$d_i = \frac{D_i}{D_M}, i = M, R; L; L, R.$$
 (SI-20)

The dimensionless concentrations:

$$q_{\rm M} = \frac{c_{\rm M}}{c_{\rm M}}, \quad q_{\rm L} = \frac{c_{\rm L}}{c_{\rm L}}, \quad q_{\rm TL} = \frac{c_{\rm T,L}}{c_{\rm T,L}}, \quad q_{\rm M} = \frac{c_{\rm R}}{c_{\rm T,R}^*}$$
 (SI-21)

With these definitions, the transport equations become:

• For the dimensionless metal:

$$\frac{\partial q_{\rm M}}{\partial t} = d_{\rm M,R} \frac{\partial^2 q_{\rm M}}{\partial z^2} - k_{\rm a} c_{\rm L}^* q_{\rm M} q_{\rm L} + k_{\rm d} \left(\frac{c_{\rm T,L}^*}{c_{\rm M}^*} q_{\rm T,L} - \frac{c_{\rm L}^*}{c_{\rm M}^*} q_{\rm L} \right) - k_{\rm a,R} c_{\rm T,R}^* q_{\rm M} q_{\rm R} + \frac{k_{\rm d,R} c_{\rm T,R}^*}{c_{\rm M}^*} (1 - q_{\rm R}), \tag{SI-22}$$

for $0 < z < r^*$, and

$$\frac{\partial q_{\mathrm{M}}}{\partial t} = \frac{\partial^2 q_{\mathrm{M}}}{\partial z^2} - k_{\mathrm{a}} c_{\mathrm{L}}^* q_{\mathrm{M}} q_{\mathrm{L}} + k_{\mathrm{d}} \left(\frac{c_{\mathrm{T,L}}^*}{c_{\mathrm{M}}^*} q_{\mathrm{T,L}} - \frac{c_{\mathrm{L}}^*}{c_{\mathrm{M}}^*} q_{\mathrm{L}} \right), \quad \text{for } r^* < z < g^*$$
(SI-23)

with initial and boundary conditions:

$$q_{\rm M}(z,0) = 0, \ \frac{\partial q_{\rm M}}{\partial z}\Big|_{z=0} = 0, \ q_{\rm M}(g^*,t) = 1,$$
 (SI-24)

$$q_{\rm M}(r^{*-},t) = q_{\rm M}(r^{*+},t), \quad d_{\rm M,R} \left. \frac{\partial q_{\rm M}}{\partial z} \right|_{z=r^{*-}} = \left. \frac{\partial q_{\rm M}}{\partial z} \right|_{z=r^{*+}}.$$
 (SI-25)

• Equations for the dimensionless ligand:

$$\frac{\partial q_{\rm L}}{\partial t} = \begin{cases} d_{\rm L,R} \\ d_{\rm L} \end{cases} \frac{\partial^2 q_{\rm L}}{\partial z^2} - k_{\rm a} c_{\rm M}^* q_{\rm M} q_{\rm L} + k_{\rm d} \left(\frac{c_{\rm T,L}^*}{c_{\rm L}^*} q_{\rm T,L} - q_{\rm L} \right), \tag{SI-26}$$

$$q_{L}(z,0) = 0, \frac{\partial q_{L}}{\partial z}\Big|_{z=0} = 0, \quad q_{L}(g^{*},t) = 1,$$
 (SI-27)

$$q_{L}(r^{*-},t) = q_{L}(r^{*+},t), \quad \frac{d_{L,R}}{d_{L}} \frac{\partial q_{L}}{\partial z} \bigg|_{z=r^{*-}} = \frac{\partial q_{L}}{\partial z} \bigg|_{z=r^{*+}}.$$
 (SI-28)

• Equations for the dimensionless total ligand:

$$\frac{\partial q_{\text{T,L}}}{\partial t} = \begin{cases} d_{\text{L,R}} \\ d_{\text{L}} \end{cases} \frac{\partial^2 q_{\text{T,L}}}{\partial z^2}, \tag{SI-29}$$

$$q_{T,L}(z,0) = 0, \frac{\partial q_{T,L}}{\partial z}\Big|_{z=0} = 0, \quad q_{T,L}(g^*,t) = 1,$$
 (SI-30)

$$q_{T,L}(r^{*-},t) = q_{T,L}(r^{*+},t), \quad \frac{d_{L,R}}{d_L} \frac{\partial q_{T,L}}{\partial z} \bigg|_{z=r^{*-}} = \frac{\partial q_{T,L}}{\partial z} \bigg|_{z=r^{*+}}.$$
 (SI-31)

• Equation for the dimensionless free resin concentration:

$$\frac{\partial q_{\rm R}}{\partial t} = -k_{\rm a,R} c_{\rm M}^* q_{\rm M} q_{\rm R} + k_{\rm d,R} (1 - q_{\rm R}), \quad \text{if } 0 < z < r^*,$$
with initial condition $q_{\rm R}(z,0) = 1$.

1.3.- Discretization

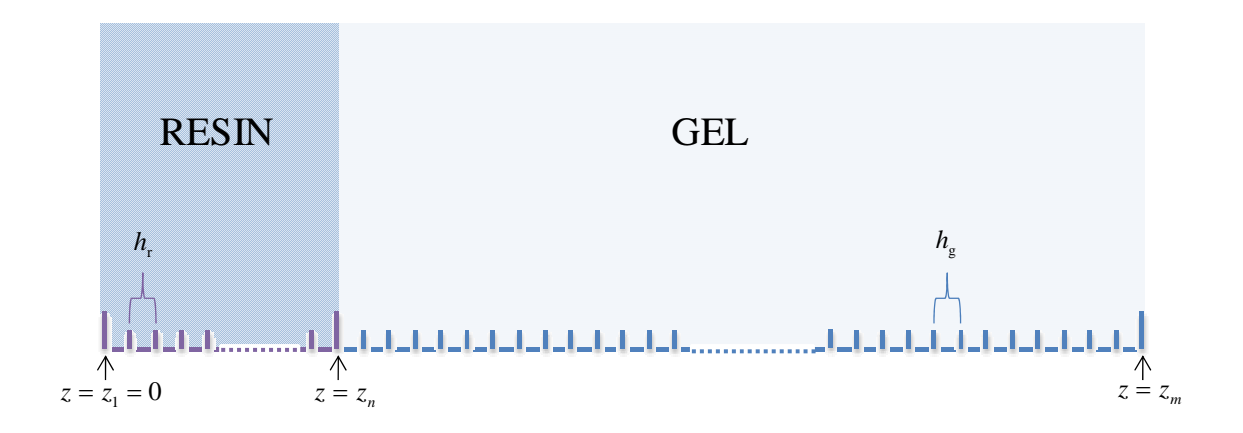


Figure SI-2. Schematic representation of spatial grid.

The resin layer domain will be divided into n-1 equal parts of length $h_r = \frac{r}{n-1}$. The gel domain will be divided into m-1 parts of length $h_g = \frac{g}{m-n-1}$ as shown in figure SI-2. The partial differential equations are discretized using spatial finite differences and a temporal Inverse-Euler scheme with constant Δt .

1.3.1.- Resin sites concentration

The discretization of equation (SI-32) becomes:

$$q_{R}(z, t + \Delta t) - q_{R}(z, t) = -\Delta t k_{a,R} c_{M}^{*} q_{M}(z, t + \Delta t) q_{R}(z, t + \Delta t) + \Delta t k_{d,R} (1 - q_{R}(z, t + \Delta t))$$
(SI-33)

which leads to:

$$q_{R}(z, t + \Delta t) = \frac{q_{R}(z, t) + \Delta t k_{d,R}}{1 + \Delta t k_{a,R} c_{M}^{*} q_{M}(z, t + \Delta t) + \Delta t k_{d,R}}$$
(SI-34)

1.3.2.- Total ligand concentration

Although equation (SI-29) could be analytically solved, its computational cost is greater than the cost of its numerical solution. The discretized form of equation (SI-29) is:

$$q_{\mathrm{T,L}}(z,t+\Delta t) - q_{\mathrm{T,L}}(z,t) = \begin{cases} \alpha_{\mathrm{L}} \\ \alpha_{\mathrm{L,R}} \end{cases} \left[q_{\mathrm{T,L}}(z+h_{i},t+\Delta t) - 2q_{\mathrm{TL}}(z,t+\Delta t) + q_{\mathrm{T,L}}(z-h_{i},t+\Delta t) \right]$$

(SI-35)

Where h_i is equal to $h_{\rm r}$ or $h_{\rm g}$ depending on the domain, $\alpha_L = d_L \Delta t / h_{\rm g}^2$ and $\alpha_{LR} = d_{LR} \Delta t / h_{\rm r}^2$.

Equation (SI-35) can be rewritten as:

$$-\left\{\begin{matrix} \alpha_{\rm L} \\ \alpha_{\rm L,R} \end{matrix}\right\} q_{\rm T,L}(z-h_i,t+\Delta t) + \left(1+2\left\{\begin{matrix} \alpha_{\rm L} \\ \alpha_{\rm L,R} \end{matrix}\right\}\right) q_{\rm T,L}(z,t+\Delta t) - \left\{\begin{matrix} \alpha_{\rm L,R} \\ \alpha_{\rm L} \end{matrix}\right\} q_{\rm T,L}(z+h_i,t+\Delta t) = q_{\rm T,L}(z,t). \tag{SI-36}$$

which enables the equation system for $q_{\text{T,L}}(z_i, t + \Delta t)$ to be built:

• For z_1 , the equation for $q_{\rm T,L}\left(z_1,t+\Delta t\right)$ is obtained from equation (SI-30), corresponding to the null flux condition at the origin,

$$q_{\text{TI}}(z_2, t + \Delta t) - q_{\text{TI}}(z_1, t + \Delta t) = 0.$$
 (SI-37)

• For j = 2 to n-1, the equations are obtained from (SI-36) considering the resin layer domain:

$$-\alpha_{\mathrm{L,R}}q_{\mathrm{T,L}}(z_{j}-h_{\mathrm{r}},t+\Delta t) + \left(1+2\alpha_{\mathrm{L,R}}\right)q_{\mathrm{T,L}}(z_{j},t+\Delta t) - \alpha_{\mathrm{L,R}}q_{\mathrm{T,L}}(z_{j}+h_{\mathrm{r}},t+\Delta t) = q_{\mathrm{T,L}}(z_{j},t)$$

$$(SI-38)$$

• At z_n , that is $z = r^*$, the equation is obtained from the boundary condition (SI-31):

$$\frac{d_{L,R}}{d_L} \frac{q_{T,L}(z_n, t + \Delta t) - q_{T,L}(z_{n-1}, t + \Delta t)}{h_r} = \frac{q_{T,L}(z_{n+1}, t + \Delta t) - q_{T,L}(z_n, t + \Delta t)}{h_g},$$
 (SI-39)

which can be rewritten as

$$-\sigma q_{T,L}(z_{n-1}, t + \Delta t) + (\sigma + 1)q_{T,L}(z_n, t + \Delta t) - q_{T,L}(z_{n-1}, t + \Delta t) = 0$$

$$h_n d_{T,R}$$
(SI-40)

where $\sigma = \frac{h_{\rm g} d_{\rm LR}}{h_{\rm r} d_{\rm L}}$

• For j = n + 1 to m - 1, we are in the gel domain and the equations for $q_{T,L}(z_i, t + \Delta t)$ are obtained from (SI-36):

$$-\alpha_{\rm L} q_{\rm T,L}(z_j - h_{\rm g}, t + \Delta t) + (1 + 2\alpha_{\rm L}) q_{\rm T,L}(z_j, t + \Delta t) - \alpha_{\rm L} q_{\rm T,L}(z_j + h_{\rm g}, t + \Delta t) = q_{\rm T,L}(z_j, t)$$
(SI-41)

• Finally, for $z = g^*$ the equation is obtained from condition in (SI-30):

$$q_{\text{TL}}(g^*, t + \Delta t) = 1 \tag{SI-42}$$

1.3.3.- Dimensionless ligand concentration

In the same way, the discretized form of equation (SI-26) is:

$$q_{L}(z,t+\Delta t) - q_{L}(z,t) = \begin{cases} \alpha_{L,R} \\ \alpha_{L} \end{cases} \left[q_{L}(z+h_{i},t+\Delta t) - 2q_{L}(z,t+\Delta t) + q_{L}(z-h_{i},t+\Delta t) \right]$$

$$-\Delta t k_{a} c_{M}^{*} q_{M}(z,t+\Delta t) q_{L}(z,t+\Delta t) + \Delta t k_{d} \frac{c_{T,L}^{*}}{c_{L}^{*}} q_{T,L}(z,t+\Delta t) - \Delta t k_{d} q_{L}(z,t+\Delta t), \qquad (SI-43)$$

or

$$-\left\{\begin{matrix} \alpha_{\mathrm{L,R}} \\ \alpha_{\mathrm{L}} \end{matrix}\right\} q_{\mathrm{L}}(z - h_{i}, t + \Delta t) + \left[1 + 2\left\{\begin{matrix} \alpha_{\mathrm{L,R}} \\ \alpha_{\mathrm{L}} \end{matrix}\right\} + \Delta t k_{\mathrm{a}} c_{\mathrm{M}}^{*} q_{\mathrm{M}}(z, t + \Delta t) + \Delta t k_{\mathrm{d}} \right] q_{\mathrm{L}}(z, t + \Delta t)$$

$$-\left\{\begin{matrix} \alpha_{\mathrm{L,R}} \\ \alpha_{\mathrm{L}} \end{matrix}\right\} q_{\mathrm{L}}(z + h_{i}, t + \Delta t) = q_{\mathrm{L}}(z, t) + \Delta t k_{\mathrm{d}} \frac{c_{\mathrm{T,L}}^{*}}{c_{\mathrm{L}}^{*}} q_{\mathrm{T,L}}(z, t + \Delta t). \tag{SI-44}$$

Particular equations for each $q_L(z_i, t + \Delta t)$ can be written.

• The first equation, for z_1 reads:

$$q_{L}(z_{2}, t + \Delta t) - q_{L}(z_{1}, t + \Delta t) = 0.$$

• From j = 2 to n-1:

$$-\alpha_{\mathrm{L,R}}q_{\mathrm{L}}(z_{j}-h_{\mathrm{r}},t+\Delta t) + \left[1+2\alpha_{\mathrm{L,R}}+\Delta t k_{\mathrm{a}}c_{\mathrm{M}}^{*}q_{\mathrm{M}}(z_{j},t+\Delta t) + \Delta t k_{\mathrm{d}}\right]q_{\mathrm{L}}(z_{j},t+\Delta t)$$

$$-\alpha_{\mathrm{L,R}}q_{\mathrm{L}}(z_{j}+h_{\mathrm{r}},t+\Delta t) = q_{\mathrm{L}}(z_{j},t) + \Delta t k_{\mathrm{d}}\frac{c_{\mathrm{T,L}}^{*}}{c_{\mathrm{t}}^{*}}q_{\mathrm{T,L}}(z_{j},t+\Delta t). \tag{SI-46}$$

• At $z = z_n = r^*$:

$$\frac{d_{L,R}}{d_L} \frac{q_L(z_n, t + \Delta t) - q_L(z_{n-1}, t + \Delta t)}{h_r} = \frac{q_L(z_{n+1}, t + \Delta t) - q_L(z_n, t + \Delta t)}{h_o},$$
(SI-47)

which rewrites as

$$-\sigma q_{L}(z_{n-1}, t + \Delta t) + (\sigma + 1)q_{L}(z_{n}, t + \Delta t) - q_{L}(z_{n-1}, t + \Delta t) = 0.$$
(SI-48)

• For j = n + 1 to m - 1:

$$-\alpha_{\rm L}q_{\rm L}(z_j - h_{\rm g}, t + \Delta t) + \left[1 + 2\alpha_{\rm L} + \Delta t k_{\rm a} c_{\rm M}^* q_{\rm M}(z_j, t + \Delta t) + \Delta t k_{\rm d}\right] q_{\rm L}(z_j, t + \Delta t)$$

$$-\alpha_{\rm L}q_{\rm L}(z_j + h_{\rm g}, t + \Delta t) = q_{\rm L}(z_j, t) + \Delta t k_{\rm d} \frac{c_{\rm T,L}^*}{c_{\rm L}^*} q_{\rm T,L}(z_j, t + \Delta t). \tag{SI-49}$$

• At $z = z_m = g^*$:

$$q_{\rm L}(z_{\rm m}, t + \Delta t) = 1. \tag{SI-50}$$

1.3.4.- Dimensionless metal concentration

Let us define $\alpha_{\rm M} = \frac{\Delta t}{\Delta x^2}$ and $\alpha_{\rm M,R} = d_{\rm M,R} \alpha_{\rm M}$.

Discretization of equation (SI-22) becomes:

$$q_{\mathrm{M}}(z_{j},t+\Delta t)-q_{\mathrm{M}}(z_{j},t)=\alpha_{\mathrm{M,R}}\left\lceil q_{\mathrm{M}}(z_{j}+h_{\mathrm{r}},t+\Delta t)-2q_{\mathrm{M}}(z_{j},t+\Delta t)+q_{\mathrm{M}}(z_{j}-h_{\mathrm{r}},t+\Delta t)\right\rceil$$

$$-\Delta t k_{\rm a} c_{\rm L}^* q_{\rm M}(z_j, t + \Delta t) q_{\rm L}(z_j, t + \Delta t) + \Delta t k_{\rm d} \frac{c_{\rm T,L}^*}{c_{\rm M}^*} q_{\rm T,L}(z_j, t + \Delta t) - \Delta t k_{\rm d} \frac{c_{\rm L}^*}{c_{\rm M}^*} q_{\rm L}(z_j, t + \Delta t) \\ -\Delta t k_{\rm a,R} c_{\rm T,R}^* q_{\rm M}(z_j, t + \Delta t) q_{\rm R}(z_j, t + \Delta t) + \Delta t k_{\rm d,R} \frac{c_{\rm T,R}^*}{c_{\rm M}^*} \Big[1 - q_{\rm R}(z_j, t + \Delta t) \Big], \tag{SI-51}$$
 and for equation (SI-23):

$$q_{\rm M}(z_{j},t+\Delta t) - q_{\rm M}(z_{j},t) = \alpha_{\rm M} \left[q_{\rm M}(z_{j}+h_{\rm g},t+\Delta t) - 2q_{\rm M}(z_{j},t+\Delta t) + q_{\rm M}(z_{j}-h_{\rm g},t+\Delta t) \right]$$

$$-\Delta t k_{\rm a} c_{\rm L}^{*} q_{\rm M}(z_{j},t+\Delta t) q_{\rm L}(z_{j},t+\Delta t) + \Delta t k_{\rm d} \frac{c_{\rm T,L}^{*}}{c_{\rm M}^{*}} q_{\rm T,L}(z_{j},t+\Delta t) - \Delta t k_{\rm d} \frac{c_{\rm L}^{*}}{c_{\rm M}^{*}} q_{\rm L}(z_{j},t+\Delta t).$$

$$(SI-52)$$

The equations for each spatial node can be constructed with the same procedure as before.

• For z_1 :

$$q_{\rm M}(z_2, t + \Delta t) - q_{\rm M}(z_1, t + \Delta t) = 0.$$
 (SI-53)

• From j = 2 to n-1:

$$\begin{split} &-\alpha_{\text{MR}}q_{\text{M}}(z_{j}-h_{\text{r}},t+\Delta t) \\ &+ \Big[1 + 2\alpha_{\text{MR}} + \Delta t k_{\text{a}} c_{\text{L}}^{*} q_{\text{L}}(z_{j},t+\Delta t) + \Delta t k_{\text{a,R}} c_{\text{T,R}}^{*} q_{\text{R}}(z_{j},t+\Delta t) \Big] q_{\text{M}}(z_{j},t+\Delta t) \\ &-\alpha_{\text{M,R}} q_{\text{M}}(z_{j}+h_{\text{r}},t+\Delta t) \\ &= q_{\text{M}}(z_{j},t) + \Delta t k_{\text{d}} \frac{c_{\text{TL}}^{*}}{c_{\text{M}}^{*}} q_{\text{T,L}}(z_{j},t+\Delta t) - \Delta t k_{\text{d}} \frac{c_{\text{L}}^{*}}{c_{\text{M}}^{*}} q_{\text{L}}(z_{j},t+\Delta t) + \Delta t k_{\text{d,R}} \frac{c_{\text{T,R}}^{*}}{c_{\text{M}}^{*}} \Big[1 - q_{\text{R}}(z_{j},t+\Delta t) \Big]. \end{split}$$

$$(\text{SI-54})$$

• At $z = z_n = r^*$:

$$d_{M,R} \frac{q_{M}(z_{n}, t + \Delta t) - q_{M}(z_{n-1}, t + \Delta t)}{h_{r}} = \frac{q_{M}(z_{n+1}, t + \Delta t) - q_{M}(z_{n}, t + \Delta t)}{h_{g}}.$$
 (SI-55)

• From j = n + 1 to m - 1:

$$-\alpha_{M}q_{M}(z_{j}-h_{g},t+\Delta t) + \left[1+2\alpha_{M}+\Delta t k_{a} c_{L}^{*} q_{L}(z_{j},t+\Delta t)\right] q_{M}(z_{j},t+\Delta t) - \alpha_{M}q_{M}(z_{j}+h_{g},t+\Delta t)$$

$$= q_{M}(z_{j},t) + \Delta t k_{d} \frac{c_{T,L}^{*}}{c_{M}^{*}} q_{T,L}(z_{j},t+\Delta t) - \Delta t k_{d} \frac{c_{L}^{*}}{c_{M}^{*}} q_{L}(z_{j},t+\Delta t).$$
(SI-56)

• At
$$z = z_{\rm m} = g^*$$
:

$$q_{\rm M}(z_{\rm m}, t + \Delta t) = 1. \tag{SI-57}$$

1.4.- Solution Procedure

The coupled system of non linear equations obtained in the previous section (equations SI-34 to SI-57) will be solved separately for each species and time. The solution is obtained after iteration and convergence of the concentration of each species at each spatial position. This method allows a extremely huge reduction of the computational time in comparison to the CPU time required for the direct solution of the non-linear system. Let us comment in more detail on the solution procedure.

The solution process begins by initializing the m+n components of vectors $\vec{q}_{T,L}, \vec{q}_L, \vec{q}_M$ and \vec{q}_R with the values reached at the previous time interval. The values of vectors $\vec{q}_{T,L}, \vec{q}_L, \vec{q}_M$ and \vec{q}_R at $t+\Delta t$ are obtained iteratively. For $q_L(z_i, t+\Delta t)$, for example, the equations system (SI-45)-(SI-50) could be rewritten in a matrix from as,

$$\begin{pmatrix} -1 & 1 & 1 \\ -a_{1R} & 1 + 2a_{1R} + \Delta t k_z \hat{c}_M q_M(z_z, t + \Delta t) + \Delta t k_d & -a_{1R} \\ & & & & & & & & & & & & & & \\ & & & & & & & & & & & & & \\ & & & & & & & & & & & & \\ & & & & & & & & & & & & \\ & & & & & & & & & & & \\ & & & & & & & & & & \\ & & & & & & & & & & \\ & & & & & & & & & & \\ & & & & & & & & & \\ & & & & & & & & \\ & & & & & & & & \\ & & & & & & & & \\ & & & & & & & \\ & & & & & & & \\ & & & & & & & \\ & & & & & & & \\ & & & & & & & \\ & & & & & & \\ & & & & & & \\ & & & & & & \\ & & & & & & \\ & & & & & & \\ & & & & & \\ & & & & & \\ & & & & & \\ & & & & & \\ & & & & & \\ & & & & & \\ & & & & \\ & & & & \\ & & & & \\ & & & & \\ & & & & \\ & & \\ & & & \\ & & \\ & & & \\$$

This is a tridiagonal system for the unknowns $q_{\rm L}(z_i,t+\Delta t)$ and it is solved iteratively through the TRIDAG.FOR subroutine (Press et al. 1986). Notice that this equation system for $q_{\rm L}$, requires the values of $q_{\rm M}(z_i,t+\Delta t)$ and $q_{\rm T,L}(z_i,t+\Delta t)$ which are also unknowns. At iteration j, to uncouple $(q_{\rm M})_j$ and $(q_{\rm T,L})_j$ from $(q_{\rm L})_j$, we use the values of both $(q_{\rm M}(z_i,t+\Delta t))_{j-1}$ and $(q_{\rm T,L}(z_i,t+\Delta t))_{j-1}$ obtained in the previous iteration (j-1) in the solution of $q_{\rm L}(z_i,t+\Delta t)$ at some iteration j. This procedure is applied iteratively for each species until all the system converges to a solution for each time step. The time is then increased and the first iteration for the next time starts initializing all the unknowns with the values obtained at the previous time.

Figure SI-3 shows schematically the algorithm used to solve the system

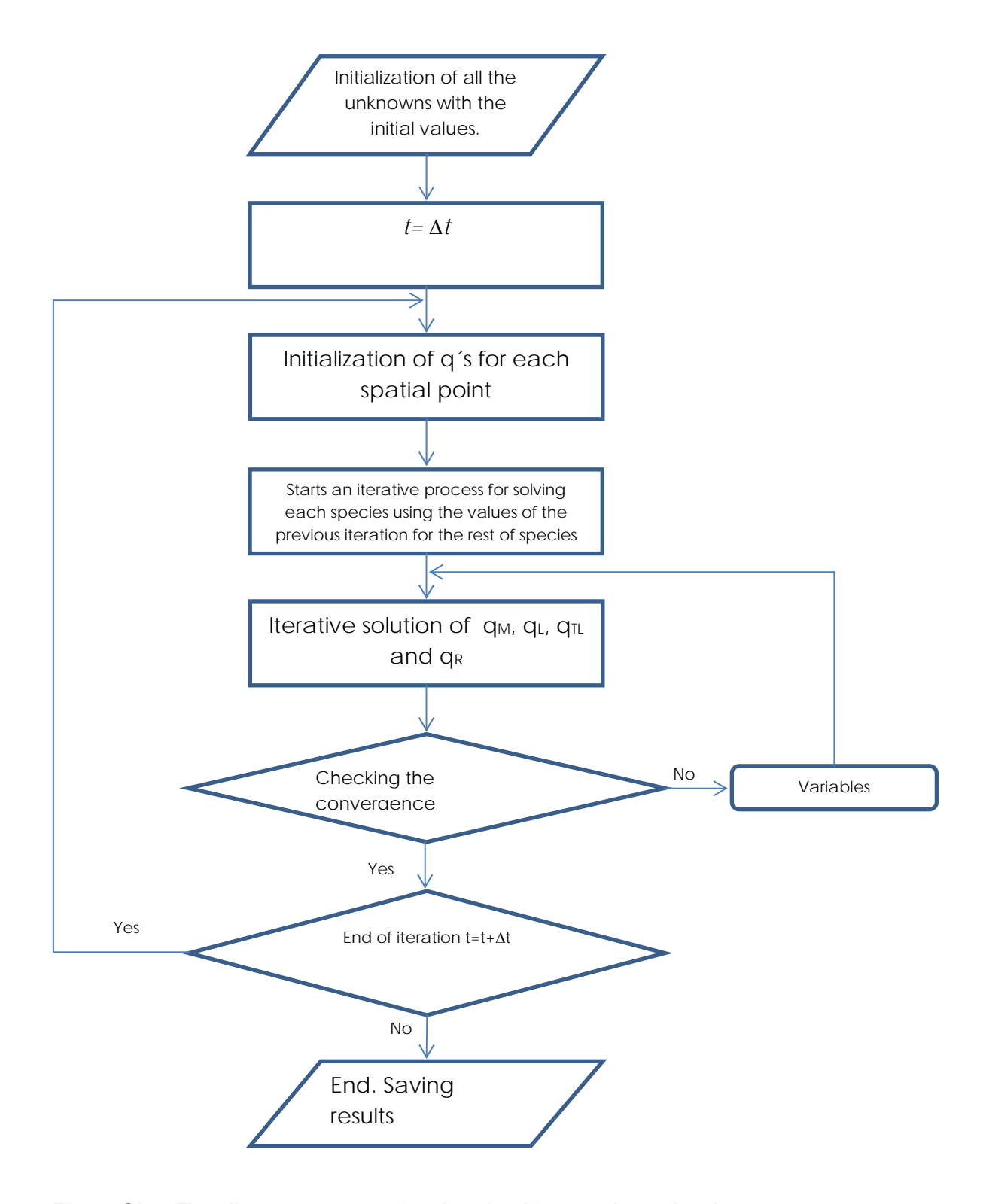


Figure SI-4. Flux diagram representing the algorithm used to solve the system

2.- Concentration profiles in a DGT experiment

Let us consider a DGT experiment using the numerical simulation described above. Fig. SI-5 depicts the concentration profiles of metal and complex through the DGT layers

and adjoining solution for different values of the kinetic complexation constants. With the parameters used in this figure, the metal concentration drops to almost zero at the resin interface due to the strong and fast resin binding. For low values of the dissociation rate constants (see panel a), the complex concentration profile is flat and equal to the complex concentration in solution, while the metal concentration profile is linear. This indicates the inert behaviour of the complex, which does not contribute to the flux received by DGT and the quasi-steady-state regime reached (the linear metal concentration profile indicates a time independent metal flux). On increasing the kinetic complexation constants (see panel b), the complex is depleted and its contribution to the metal flux through dissociation is apparent. Notice that the metal concentrations do not increase linearly with distance and their values at a given x are greater than those of the inert case, due to the complex dissociation contributing to a higher local metal concentration. A further increase of the kinetic constants leads to a more depleted complex concentration profile. Metal and complex concentration profiles increasingly coincide in the gel domain (see panel c). When both normalised profiles coincide, metal and complex are in local equilibrium, indicating that the complex is able to dissociate sufficiently rapidly to maintain equilibrium conditions with the metal. The thickness of the layer where both profiles diverge, can be related to the reaction layer. As expected, the thickness of the reaction layer decreases as the kinetic constants increase. Notice that at the interface between the resin and gel layers the slope of the complex concentration profile is not zero and the complex penetrates into the resin layer. The decrease in the complex concentration as the back plastic wall of the device is approached continues inside the resin, indicating that the dissociation process does not cease at the resin interface. A further increase of the kinetic constants (see panel d) leads to linear metal and complex concentration profiles superimposed throughout the entire

gel domain. This corresponds to the labile situation where the dissociation of the complex is so fast that local equilibrium with the metal is reached at each relevant spatial and time position.

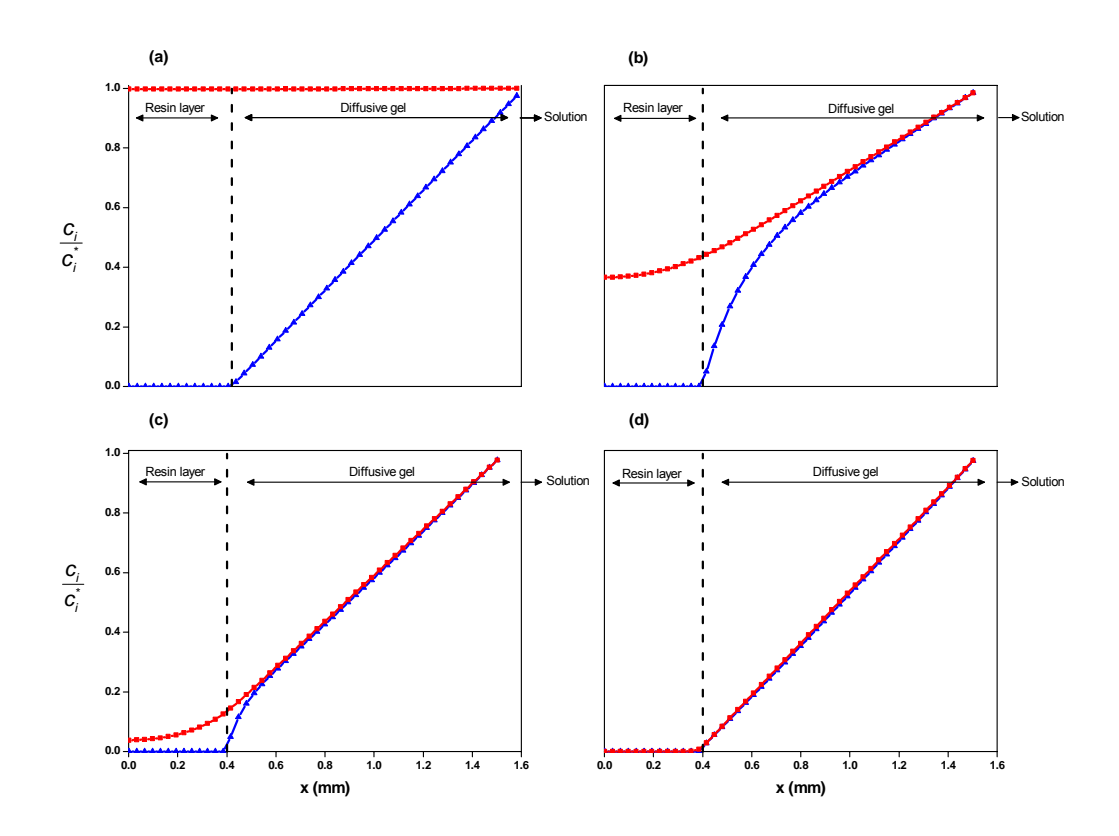


Figure SI-5. Normalized concentration profiles of M (Blue line with \triangle markers) and ML (red line with \blacksquare markers). Profiles are obtained by numerical simulation described in SI-1. Parameters: $r = 4 \times 10^{-4} \, \mathrm{m}$, $K = 10^2 \, \mathrm{mol}^{-1} \, \mathrm{m}^3 \, \mathrm{s}^{-1}$, panel a): $k_{\mathrm{d}} = 10^{-6} \, \mathrm{s}^{-1}$, panel b) $k_{\mathrm{d}} = 10^{-3} \, \mathrm{s}^{-1}$, panel c) $k_{\mathrm{d}} = 10^{-2} \, \mathrm{s}^{-1}$ and panel d) $k_{\mathrm{d}} = 10^0 \, \mathrm{s}^{-1}$. The rest of parameters as in figure 1 of the manuscript.

3.- Experimental Section

DGT sensors

All DGT sensors were purchased from DGT Research Ltd. (Lancaster, U.K.). Commercially available DGT deployment mouldings made of ABS polymer, based on a simple, tight-fitting piston design with a 2 cm diameter window, were used for all

measurements. A 0.4 mm thick Chelex-gel was placed on the piston surface with the side packed with resin beads facing upward (i.e. in close contact with the diffusive layer). On the top of the Chelex-gel, a 0.8 mm thick diffusive agarose polyacrylamide gel and a cellulose nitrate membrane (Whatman, pore size 0.45 µm, thickness 0.125 mm) were placed. A more detailed description is found at DGT Research's homepage (http://www.dgtresearch.com).

• DGT Experiments

A series of experiments were performed to determine the mass of cadmium accumulated at different times by DGT devices deployed in solutions containing Cd (prepared from the solid nitrate product, Merck, analytical grade) at a concentration close to $10^{-2} \, \text{mol m}^{-3}$ and NTA (Fluka, analytical grade) at concentrations of 0.249 and $1.8 \, \text{mol m}^{-3}$. pH was adjusted by means of small additions of NaOH or HNO₃ to 7 or 7.5 before and during the deployment. Ionic strength of the solution was adjusted to $0.05 \, \text{mol L}^{-1}$ with NaNO₃ (Merck, suprapur). Ultra-pure water (Mill-Q plus 185 System, Millipore) was employed in all the experiments.

• DGT Exposure Chamber

A 5L polyethylene bucket was used as the exposure chamber. 11 DGTs were fixed by press-stud. pH was monitored continuously with a glass electrode. A reference electrode Ag/AgCl/3 mol.L⁻¹ KCl, with a 0.05 mol.L⁻¹ NaNO₃ jacket was used. The exposure chamber was placed in a thermostated bath to keep the deployment solution at constant temperature of 25±0.1°C. The solution was stirred during deployment using an overhead stirrer.

• Retrieval and analysis

For all experiments, aliquots of the solution were collected at regular intervals to check the total Cd concentration. DGT devices, once removed from solution, were rinsed with ultrapure water and opened for removal of the resin gels, which were then eluted in 1mL of concentrated nitric acid for at least 24h. The number of moles of metal in the form of non dissociated complex due to the complex penetration into the resin domain is negligible in comparison with those bound to the resin beads All solutions were analysed by inductively coupled plasma-optical emission spectroscopy (ICP-OES) (Activa-S, Horiba Scientific).

4.- Additional figures

Additional figures that verified the influence of the thickness of the DGT resin layer on the accumulated mass for the Cd-NTA system.

Conditional stability constants and kinetic parameters for the Cd NTA system at a given pH, ionic strength and total metal and total ligand concentration were estimated as reported in the manuscript. Values used in the numerical simulations for the kinetic association and dissociation constants of the metal to the resin sites are $k_{\rm a,R}=10^{15}\,{\rm mol^{-1}\,m^3s^{-1}} \ {\rm and} \ k_{\rm d,R}=10^{-6}\,{\rm s^{-1}} \ {\rm while} \ {\rm the total} \ {\rm concentration} \ {\rm of} \ {\rm resin} \ {\rm sites} \ {\rm in} \ {\rm the} \ {\rm resin} \ {\rm layer} \ {\rm is} \ c_{\rm T,R}=50\,{\rm mol}\,{\rm m^{-3}} \ .$ These values are high enough to neglect saturation effects and to reach an almost null metal concentration at the resin interface.

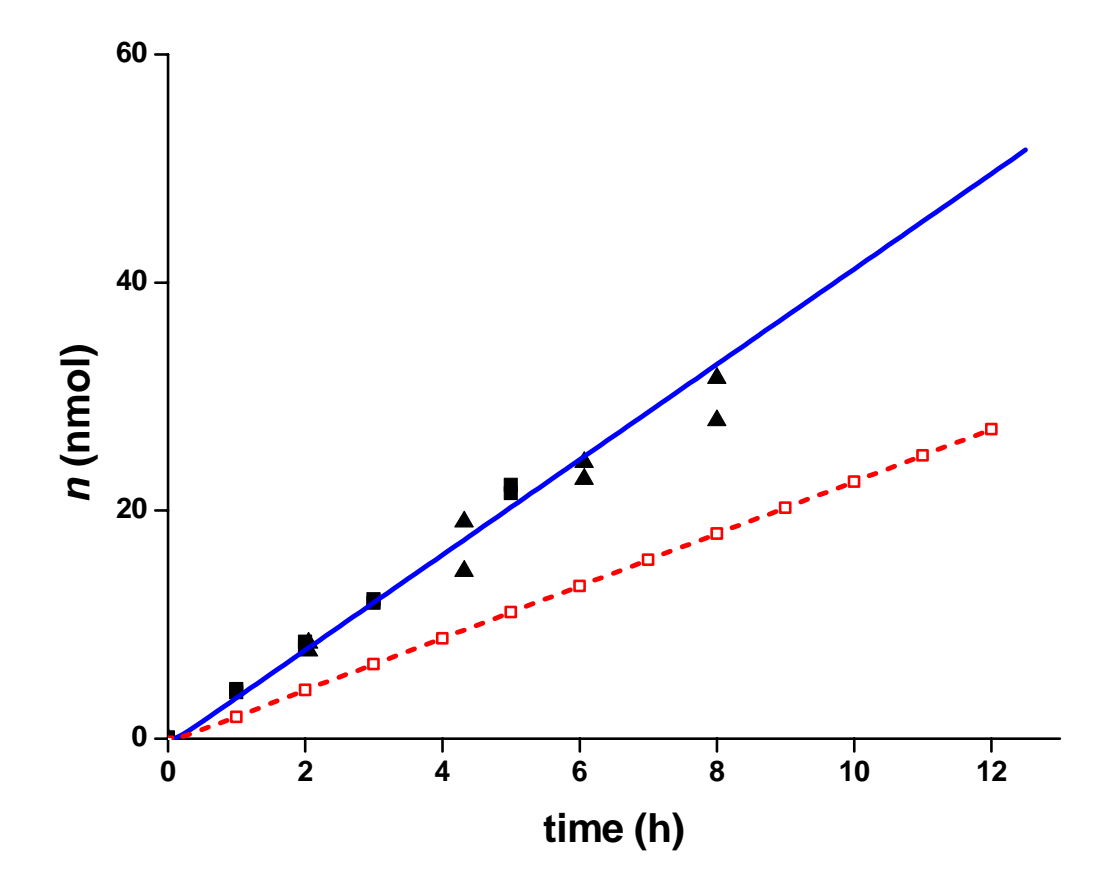


Figure SI-6. Moles of Cd accumulated by DGT in presence of NTA. Markers: experimental measurements, two deployments (\blacksquare) and (\blacktriangle). Blue continuous line: theoretical accumulation predicted by numerical simulation when penetration of the complex into the resin layer is considered ($r=4\times10^{-4}\,\mathrm{m}$). Red dashed line with markers \Box : theoretical accumulation predicted by numerical simulation when penetration of the complex into the resin layer is not allowed (r=0). Parameters: total NTA concentration $c_{\mathrm{T,NTA}}=0.249\,\mathrm{mol\,m^{-3}}$, total Cd concentration $c_{\mathrm{T,Cd}}=9.96\times10^{-3}\,\mathrm{mol\,m^{-3}}$, pH=7.03, I=0.05M, $k_{\mathrm{a}}^{\mathrm{eff}}=8.77\times10^{4}\,\mathrm{m^{3}mol^{-1}s^{-1}}$ and $k_{\mathrm{d}}=k_{\mathrm{d}}^{\mathrm{eff}}=\frac{k_{\mathrm{a}}^{\mathrm{eff}}}{K_{\mathrm{CdNTA}}^{\mathrm{eff}}}=2.76\,\mathrm{s^{-1}}$. The rest of parameters as in figure 4 of the manuscript.

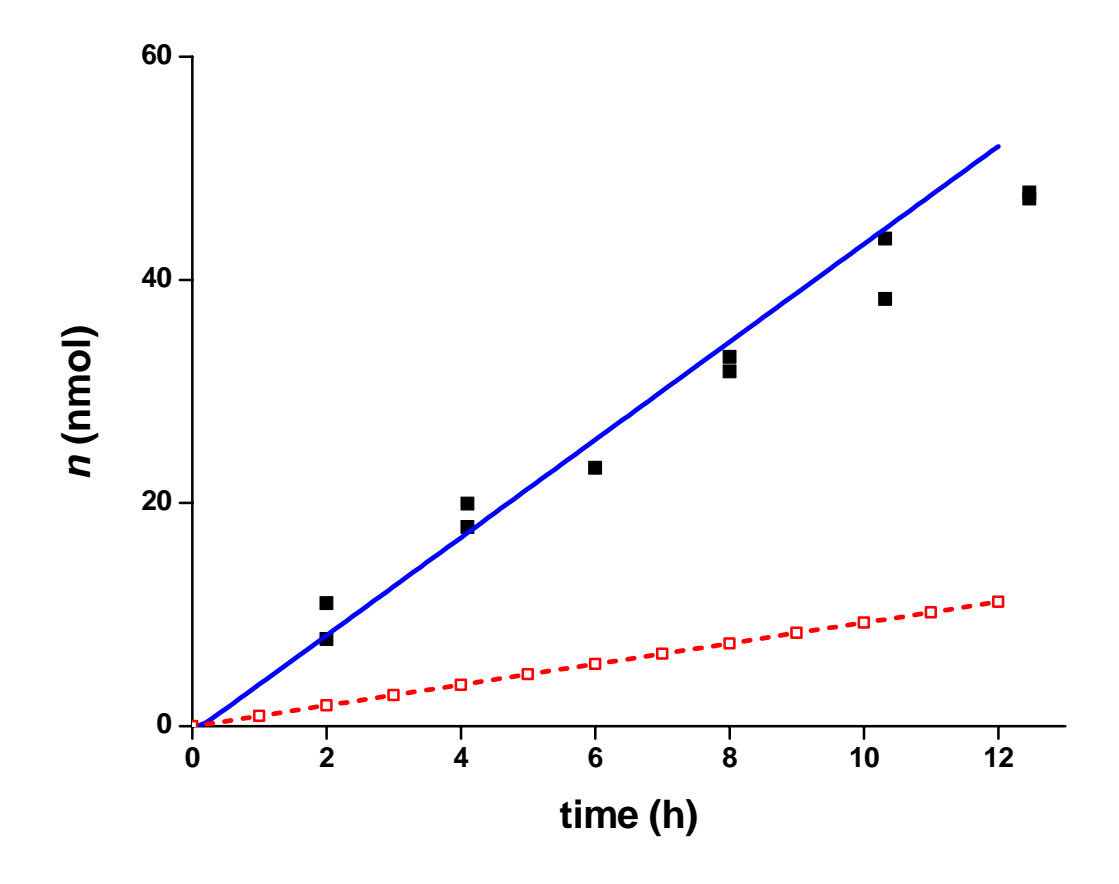


Figure SI-7. Moles of Cd accumulated by DGT in presence of NTA. Marker (\blacksquare): experimental measurements. Blue continuous line: theoretical accumulation predicted by numerical simulation when penetration of the complex into the resin layer is considered ($r=4\times10^{-4}\,\mathrm{m}$). Red line with markers \Box : theoretical accumulation predicted by numerical simulation when penetration of the complex into the resin layer is not allowed (r=0). Parameters: total NTA concentration $c_{\mathrm{T,NTA}}=1.8\,\mathrm{mol}\,\mathrm{m}^{-3}$, total Cd concentration $c_{\mathrm{T,Cd}}=1.08\times10^{-2}\,\mathrm{mol}\,\mathrm{m}^{-3}$, pH=7.50,ionic strength 0.05M, $k_{\mathrm{a}}^{\mathrm{eff}}=2.58\times10^{5}\,\mathrm{m}^{3}\mathrm{mol}^{-1}\mathrm{s}^{-1}$ and $k_{\mathrm{d}}=k_{\mathrm{d}}^{\mathrm{eff}}=\frac{k_{\mathrm{a}}^{\mathrm{eff}}}{K_{\mathrm{CdNTA}}^{\mathrm{eff}}}=2.76\,\mathrm{s}^{-1}$. The rest of parameters as in figure 4 of the manuscript.

5.- Formulation of the Cd-NTA speciation in a DGT sensor as a system with only one complex and ligand species.

NTA is involved in four acid-base equilibria. Among all these species only NTA³⁻ is known to interact with Cd to give the complex species CdNTA and Cd(NTA)₂. Thus only NTA³⁻ is the ligand in the Cd-NTA system. However, the concentration of NTA³⁻ is not only modified by the presence of Cd, but also by the pH of the system. The formulation of the Cd-NTA system as

$$M + L \stackrel{k_{a,L}}{\leftarrow} ML$$
 (SI-59)

with a fixed total ligand concentration, $c_{\rm T,L}$, computed as $c_{\rm T,L} = c_{\rm L} + c_{\rm M,L}$ is then not valid. It is the aim of this section of this supporting information to show that the Cd-NTA system can be reformulated so that equations equivalent to the system represented with scheme SI-60 can be applied.

Let us assume that

- i) protonated and unprotonated NTA species have the same diffusion coefficient, $D_{\rm L}$
- ii) the kinetics of interconversion between the protonated/unprotonated NTA species is considered instantaneous (i.e. they are always at equilibrium), so that all the protonated and unprotonated species diffuse and react as one "single species".

A scheme of the processes in solution is:

$$\begin{array}{c} M+L & \xrightarrow{k_{a,L}} & ML \\ \\ + \\ H \\ k_{d1,H} & \uparrow \downarrow k_{a1,H} \\ \\ + \\ HL \\ + \\ + \\ H \\ k_{d2,H} & \uparrow \downarrow k_{a2,H} \\ \\ \dots \\ \\ H_4L \end{array} \tag{SI-60}$$

The transport problem can be stated as

$$\frac{\partial c_{\rm M}}{\partial t} = D_{\rm M} \frac{\partial^2 c_{\rm M}}{\partial x^2} + k_{\rm d,L} c_{\rm ML} - k_{\rm a,L} c_{\rm M} c_{\rm L}$$
(SI-61)

$$\frac{\partial c_{\text{ML}}}{\partial t} = D_{\text{L}} \frac{\partial^2 c_{\text{ML}}}{\partial x^2} - k_{\text{d,L}} c_{\text{ML}} + k_{\text{a,L}} c_{\text{M}} c_{\text{L}}$$
(SI-62)

$$\frac{\partial c_{\rm L}}{\partial t} = D_{\rm L} \frac{\partial^2 c_{\rm L}}{\partial x^2} + k_{\rm d,L} c_{\rm M,L} - k_{\rm a,L} c_{\rm M} c_{\rm L} + k_{\rm d1,H} c_{\rm HL} - k_{\rm a1,H} c_{\rm H} c_{\rm L}$$
(SI-63)

$$\frac{\partial c_{\text{HL}}}{\partial t} = D_{\text{L}} \frac{\partial^2 c_{\text{HL}}}{\partial x^2} + k_{\text{d2,H}} c_{\text{H_2L}} - k_{\text{a2,H}} c_{\text{H}} c_{\text{HL}} - k_{\text{d1,H}} c_{\text{HL}} + k_{\text{a1,H}} c_{\text{H}} c_{\text{L}}$$
(SI-64)

. . . .

$$\frac{\partial c_{H_4L}}{\partial t} = D_L \frac{\partial^2 c_{H_4L}}{\partial x^2} - k_{d4,H} c_{H_3L} + k_{a4,H} c_{H_3L}$$
 (SI-65)

Adding the transport Eqns. of all the protonated ligand forms (Eqns. (SI-63)-(SI-65))

$$\frac{\partial c_{L,P}}{\partial t} = D_L \frac{\partial^2 c_{L,P}}{\partial x^2} + k_{d,L} c_{ML} - k_{a,L} c_M c_L$$
 (SI-66)

where $c_{\mathrm{L.P}}$ stands for

$$c_{L,P} = c_L + c_{HL} + c_{H_2L} + c_{H_3L} + c_{H_4L}$$
 (SI-67)

Since protonation is instantaneous, acid-base equilibria relationship apply:

$$\beta_{i,H} = \frac{c_{H_i L}}{c_H^i c_L}$$
 (SI-68)

 $c_{\rm L}\,$ can be rewritten as

$$c_{\rm L} = \frac{c_{\rm L,P}}{1 + \sum_{i=1}^{4} \beta_{i,\rm H} c_{\rm H}^{i}}$$
 (SI-69)

In terms of $\,c_{\rm L,P}^{}$, Eqns. (SI-61), (SI-62) and (SI-66) become

$$\frac{\partial c_{\mathrm{M}}}{\partial t} = D_{\mathrm{M}} \frac{\partial^2 c_{\mathrm{M}}}{\partial x^2} + k_{\mathrm{d,L}} c_{\mathrm{ML}} - \frac{k_{\mathrm{a,L}}}{1 + \sum_{i=1}^4 \beta_{i,\mathrm{H}} c_{\mathrm{H}}^i} c_{\mathrm{M}} c_{\mathrm{L,P}}$$
(SI-70)

$$\frac{\partial c_{\text{ML}}}{\partial t} = D_{\text{L}} \frac{\partial^2 c_{\text{ML}}}{\partial x^2} - k_{\text{d,L}} c_{\text{ML}} + \frac{k_{\text{a,L}}}{1 + \sum_{i=1}^4 \beta_{i,\text{H}} c_{\text{H}}^i} c_{\text{M}} c_{\text{L,P}}$$
(SI-71)

and

$$\frac{\partial c_{\text{L,P}}}{\partial t} = D_{\text{L}} \frac{\partial^2 c_{\text{L,P}}}{\partial x^2} + k_{\text{d,L}} c_{\text{ML}} - \frac{k_{\text{a,L}}}{1 + \sum_{i=1}^4 \beta_{i,\text{H}} c_{\text{H}}^i} c_{\text{M}} c_{\text{L,P}}$$
(SI-72)

Eqns. (SI-70)-(SI-72) are formally identical to a system with one ligand with concentration $c_{\rm L,P}$, that is not involved in any protonation equilibria. The effective association and dissociation constants of this ligand with the metal are

$$k_{\rm d}^{\rm eff} = k_{\rm d,L} \tag{SI-73}$$

and

$$k_{\rm a}^{\rm eff} = \frac{k_{\rm a,L}}{1 + \sum_{i=1}^{4} \beta_{i,H} c_{\rm H}^{i}}$$
 (SI-74)

The effective stability constant of the metal complexation with this formal ligand $c_{\rm L,P}$, of concentration given by Eqn (SI-67), is

$$K^{\text{eff}} = \frac{k_{\text{a}}^{\text{eff}}}{k_{\text{d}}^{\text{eff}}} = \frac{K}{1 + \sum_{i=1}^{4} \beta_{i,\text{H}} c_{\text{H}}^{i}}$$
 (SI-75)

6.- Parameter values in all the figures of the manuscript

Table SI-1

Parameter		Fig. 1	Fig. 2	Fig. 3	Fig. 4	Units
Resin thickness	r			4×10 ⁻⁴		m
Gel thickness	g	1.13×10 ⁻³	1.13×10 ⁻³		1.13×10 ⁻³	m
Stability constant	К	10 ²	10 ²		10 ²	mol ⁻¹ m ³
Association rate constant between M and L	k _a		10 ⁻¹		2.58×10 ⁵	mol ⁻¹ m ³ s ⁻¹
Dissociation rate constant between M and L	k _d		10^{-3}		2.76	S-1
Association rate constant between M and R	k _{a,R}	10 ¹⁵	10 ¹⁵	10 ¹⁵	10 ¹⁵	mol ⁻¹ m ³ s ⁻¹
Dissociation rate constant between M and R	k d,R	10 ⁻⁶	10^{-6}	10^{-6}	10^{-6}	S-1
Diffusion coefficient of M in resin and gel	D _M D _{M,R}	6.09×10 ⁻¹⁰	6.09×10 ⁻¹⁰	6.09×10 ⁻¹⁰	6.09×10 ⁻¹⁰	m ² s ⁻¹
Diffusion coefficient of L in the resin and gel domains	D _L D _{L,R}	4.26×10 ⁻¹⁰ D _{L,R} =D _L	4.26×10^{-10} $D_{L,R} = D_L$		4.26×10 ⁻¹⁰ D _{L,R} =D _L	m ² s ⁻¹
Diffusion coefficients of ML in resin and gel	D _M L D _M L,R	4.26×10 ⁻¹⁰ <i>D</i> _{ML,R} = <i>D</i> _{ML}	4.26×10 ⁻¹⁰		4.26×10 ⁻¹⁰	m ² s ⁻¹
Total concentration of M	<i>С</i> т,м	0.01	0.01		1.08×10 ⁻²	mol m ⁻³

Total	C _{T,L}	0.249	0.249		0.249	mol m ⁻³
concentration						
of L						
			7.0	7.0		
Total	<i>C</i> T,R	50	50	50	50	mol m ⁻³
concentration						
of R						
				2 2 2		
Ionic strength	/			0.05	50	M
рН					7.50	

All simulations in this manuscript were calculated with a spatial grid of 2000 points and a time interval $\Delta t = 0.1$ s.

Literature Cited

- 1. Lehto, N. J., W. Davison, H. Zhang, and W. Tych. 2006. An evaluation of DGT performance using a dynamic numerical model. *Environmental Science and Technology* 40:6368-6376.
- 2. Press, W. H., B. P. Flannery, S. A. Teukolsky, and W. T. Vetterling. 1986. *Numerical Recipes*. Cambridge: Cambridge University Press.
- 3. Tusseau-Vuillemin, M. H., R. Gilbin, and M. Taillefert. 2003. A dynamic numerical model to characterize labile metal complexes collected with diffusion gradient in thin films devices. *Environmental Science and Technology* 37:1645-1652.